Inverse solution to the heat transfer coefficient for the oxidized ARMCO steel plate cooling by the air nozzle from high temperature

K. Jasiewicz*, Z. Malinowski† and A. Cebo-Rudnicka†

*Faculty of Metals Engineering and Industrial Computer Science
Department of Heat Engineering and Environment Protection
AGH University of Science and Technology
Cracow, Poland
e-mail: kjasiewi@agh.edu.pl

†Faculty of Metals Engineering and Industrial Computer Science
Department of Heat Engineering and Environment Protection
AGH University of Science and Technology
Cracow, Poland
e-mail: malinows@agh.edu.pl, cebo@agh.edu.pl

Key words: Inverse heat conduction problem, Finite Element Method, Air nozzle, Heat flux, Heat transfer coefficient

Abstract: *The inverse solution to the heat conduction equation for the heat transfer coefficient have been performed to the experimental data obtained during the oxidised Armco steel plate cooling by the air nozzle. A 3D numerical model of the heat transfer during the plate cooling has been considered. Steel products cooled in air from high temperatures are covered with the oxide layer having significantly lower conductivity, and a different surface structure comparing to the non-oxidised metal surface. The Armco steel has been selected as the experimental material because it oxidized in a similar way to carbon steels, but there is no microstructure evolution process in Armco steel below* $900°C$*. It eliminates in the inverse solutions serious problems caused by a latent heat of microstructure evolutions encountered during carbon steel cooling. In the present, study the steel plate has been heated to about* $900°C$ *and cooled by the air nozzle. The plate temperature has been measured by 36 thermocouples.*

1 INTRODUCTION

Air cooling is one of the most common methods of removing excess of heat from an object heated to high temperature. The heat transfer during this process consists of convection and radiation. During cooling with a stream of air, heat is mainly removed from the surface by forced convection. Under natural convection in air, the radiation part of heat transfer in the total heat flux increases. Due to the availability and high costs of obtaining other gaseous coolants, air is used most often. Cooling with a stream of air is used in the metallurgical industry, among others, during hot forging, rolling or heat treatment of metals. Air stream cooling is commonly used to cool turbines components [1]. To achieve the appropriate cooling parameters, and hence the appropriate properties of products, it is necessary to know a rate of heat removal from the surface during the cooling process. Due to the limited possibility of using other methods, especially in high-temperature processes, in order to determine the heat transfer between the coolant and the cooled surface, the inverse problem for the heat conduction equation is usually used [2, 3]. This method relies on temperature measurements at a few points inside the sample, which are then used in numerical calculations. The results of numerical calculations allow to determine the heat transfer on the cooled surface. To be able to perform numerical calculations, it is necessary to develop a heat transfer model. Mathematical and numerical models describing the heat transfer during cooling with an air stream were developed and improved by many scientists. One of the first was Beck [4]. Back presented an inverse method, by means of which, determined changes in the heat flux at the sample

https://doi.org/10.4995/YIC2021.2021.12344

surface from the temperature measurements inside a cooled copper sensor. Malinowski et al. [5] introduced an inverse method to determine three-dimensional heat transfer coefficient and heat flux as functions of time and location. Haw-Long et al. [6] presented an inverse algorithm for the solution of the inverse hyperbolic heat conduction problem. A significant problem during cooling of iron-containing products is the formation of a layer of scale on the surface. Scale formed on the cooled surface changes the heat transfer between the cooling medium and the cooled surface. Determining the thickness and properties of the scale layer formed on the surface, is important to obtain high accuracy numerical model. Li et al. [7] published the results of research concerning the thermal conductivity and diffusivity determination as temperature functions for FeO oxide. An example of a material where the problem of scale formation is significant is Armco steel. This material is used, inter alia, in the production of magnetically active parts of electrical devices in the petrochemical, energy, and shipbuilding industries. Maachou et al. [8] has tested an identification method using Volterra series to model a thermal diffusion in an Armco steel sample. The main purpose of the article is to identify the boundary conditions of heat transfer on the plate surface made of Armco steel during cooling with an air stream. The inverse method was used to determine the boundary conditions. Experimental tests were carried out, consisting of measuring the temperature inside the plate with 36 thermocouples. Temperature measurements taken during cooling were then implemented in a numerical program. The inverse solution for the heat conduction equation allowed to determine the heat transfer coefficient at the plate surfaces cooled by the air stream.

2 GENERAL SPECIFICATIONS

To identify the boundary conditions of heat transfer on the surface of the plate subjected to air cooling, it was necessary to measure the temperature change inside the plate during cooling. These measurements were carried out on an experimental stand, which consisted of three main parts: electric resistant furnace, a cooling chamber, and the temperature acquisition system. The experimental stand was equipped with a control system that allows to operate the feeder arm, furnace door, start cooling, and set furnace temperature (Fig. 1). The first stage of experimental measurements involved heating the plate in an electric furnace. The purpose of the heating was to obtain uniform temperature of about 900°C throughout the entire volume of the plate. After reaching the pre-set temperature, the plate was transported to the cooling chamber, where it was cooled by the MNM type air nozzle. The distance between the nozzle and the plate was 0,15 m. The furnace and the cooling chamber were separated by an automatic door. The plate was mounted vertically in the pneumatic feeder arm which was responsible for its transport between the furnace and the cooling chamber.

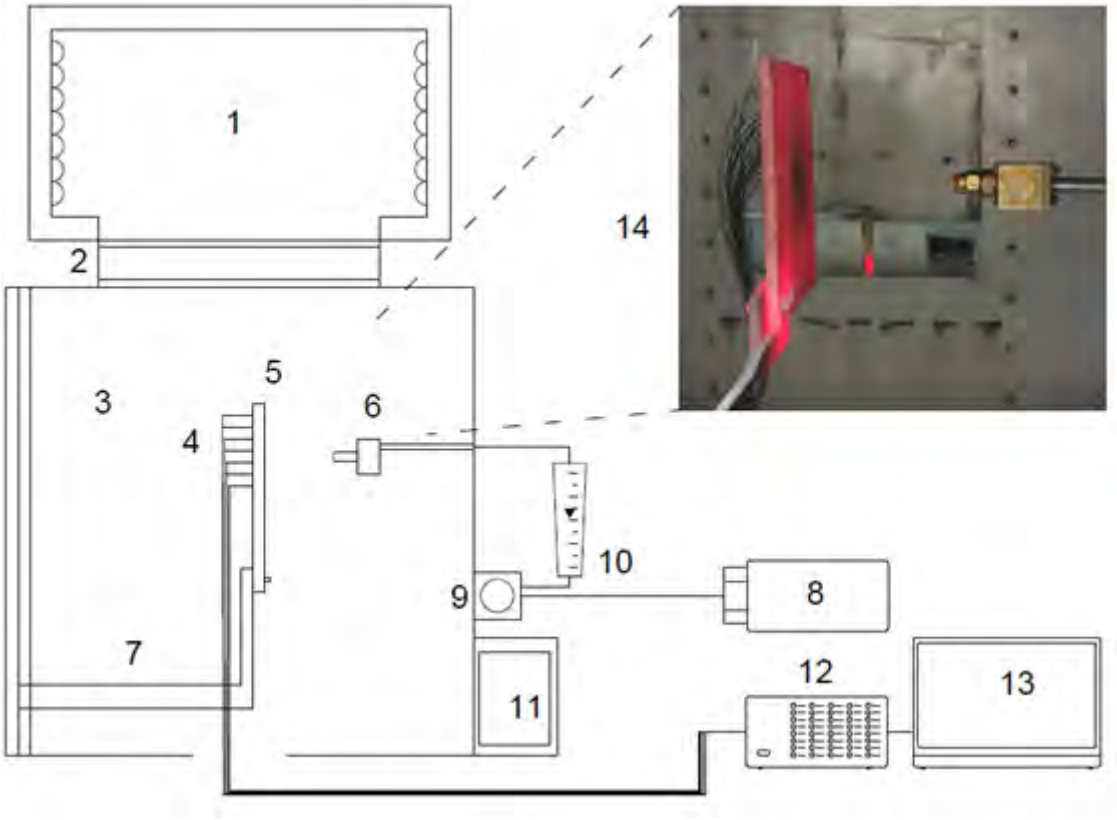

Figure 1: Experimental stand scheme. 1- electric furnace, 2- furnace door, 3- cooling chamber, 4- termocouples, 5- plate, 6- air nozzle, 7- feeder arm, 8- air compressor, 9- air pressure regulator, 10- rotameter, 11- control system, 12-temperature acquisition system, 13- laptop, 14- Armco steel plate cooled by air nozzle.

Experimental studies were carried out on a plate made of Armco steel Fig.1. The plate was $B = 10mm$ thick, $L = 245mm$ in length, and $H = 200mm$ in height. The temperature inside the plate was measured with 36 NiCr - NiAl (K type) thermocouples with a diameter of 1 mm. Thermocouples were numbered from P1 to P36. All thermocouples were placed 2 mm below the cooled surface, in holes 1 mm in diameter. The thermocouples were placed on a quarter of plate with a length of 90 mm. The arrangement of thermocouples is shown in (Fig. 4). The maximum temperature measurement error, related to the accuracy class of the thermocouple was 0.4% of the measured temperature [9]. The maximum temperature of the plate during the tests was $914°C$. It follows that the maximum temperature measurement error resulting from the accuracy class of the thermocouple was $3.66°C$. The temperature measured by the thermocouples was read with a data acquisition system [10]. The accuracy of the device was 0.2%, which means that the maximum reading error was $1.83°C$. These two sources of errors related to the temperature measurements gave the maximum temperature measurement error of about $5.5°C$. Additionally, three thermocouples were used to measure the temperature changes of the cooling chamber wall, and one thermocouple to measure the temperature of air supplied through the nozzle. Parameters of the cooling process has been presented in Table 1. The air flow during the cooling process was recorded by a rotameter.

Material	Air pressure	Distance between nozzle and plate	Cooling time	Average air temperature	Air flow
	[MPa]	[m]	[s]	[$^{\circ}C$]	[l/min]
Armco	0.1	0.15	2000	23.5	27.7

Table 1: Parameters of the cooling process.

3 THE INVERSE PROBLEM FORMULATION

The plate temperature $T(x_1, x_2, x_3, \tau)$ has been calculated from the finite element solution to the heat conduction equation:

$$\frac{\partial}{\partial x_1}\left(\lambda\frac{\partial T}{\partial x_1}\right)+\frac{\partial}{\partial x_2}\left(\lambda\frac{\partial T}{\partial x_2}\right)+\frac{\partial}{\partial x_3}\left(\lambda\frac{\partial T}{\partial x_3}\right)-\rho c\frac{\partial T}{\partial \tau}=0 \tag{1}$$

where:
c – Specific heat $[J/(kg\cdot K)]$,
T – Temperature $[^{\circ}C]$,
x_1, x_2, x_3 – Cartesian coordinates $[m]$,
λ – Thermal conductivity, $[W/(m\cdot K)]$,
ρ – Density $[kg/m3]$,
τ – Time $[s]$.

In the heat conduction model the thermal conductivity, and specific heat dependence on temperature has been considered for material selected for the experiments. The data given in [11] have been approximated with the polynomials (Fig. 2-3).

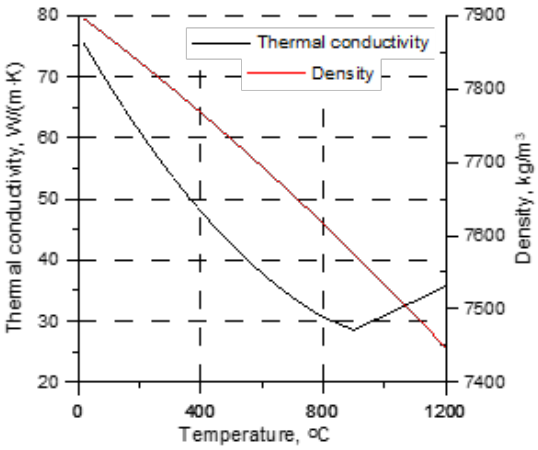

Figure 2: Thermal conductivity and density of Armco steel.

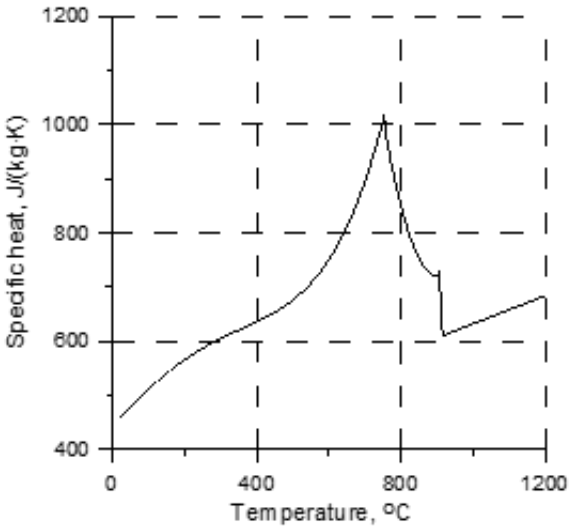

Figure 3: Specific heat of Armco steel.

A FEM algorithm and software developed by Malinowski et al. [5], has been employed to solve Eq. (1). In the FEM solution to Eq. (1) 600 elements with linear shape functions were employed. In the thickness of the plate 6 elements have been employed. The first layer of elements at the surface cooled by the nozzle had the thermophysical properties of iron oxide and a thickness of 0,097 mm. Thickness of the scale layer was determined based on measurements made after the end of the experiment. The properties of the scale implemented in numerical code were taken from Li et al. [7]. Since, the air nozzle was located in the center of the plate, and due to symmetry of the air flow, zero heat fluxes have been assumed at the two symmetry planes:

$$\dot{q}\left(x_1; x_2 = 0; x_3\right) = -\lambda \frac{\partial T}{\partial x_2} = 0 \tag{2}$$

$$\dot{q}\left(x_1; x_2; x_3 = 0\right) = -\lambda \frac{\partial T}{\partial x_3} = 0 \tag{3}$$

At the plate edges, and the vertical surfaces of the plate the boundary conditions have been approximated using the heat flux model:

$$\dot{q}_i = 5.67 \cdot 10^{-8} \frac{\left[T_s(x_1; x_2; x_3)\right]^4 - \left[T_c(\tau)\right]^4}{\frac{1}{\varepsilon_s(T)} + \frac{S_s}{S_c}\left(\frac{1}{\varepsilon_c} - 1\right)} + \propto_i \left[T_s(x_1; x_2; x_3) - T_a\right] \tag{4}$$

where:
$\dot{q}_i$ – Heat flux $[J/(kg \cdot K)]$,
S_c –Cooling chamber surface $[m^2]$,
S_s – Plate surface $[m^2]$,
T_a – Ambient temperature $[^\circ C]$,
T_c – Chamber temperature $[^\circ C]$,
T_s – Cooled surface temperature $[^\circ C]$,
ε_c – Emissivity of the cooling chamber surface,
ε_s – Emissivity of the plate surface,
$\propto_i$ – Heat transfer coefficient $[W/(m^2 \cdot K)]$.

The first term in Eq. (4) describes the radiation heat losses to the chamber walls. The cooling chamber was made of a stainless steel and had the surface $S_c = 4.33m^2$. Comparing the chamber temperature measurements given by the thermal camera with thermocouple's indications, the chamber emissivity $\varepsilon_c = 0.2$ was specified in the boundary condition model. The chamber surface temperature $T_c(\tau)$ was specified based on the thermocouple indications. The sample surface was $S_s = 0.107m^2$. The symbol i denotes a surface number at which a convection heat transfer coefficient α_i was calculated.

At the horizontal edge of the plate cooled from above the heat transfer coefficient (HTC) was calculated from the Nusselt number formula given by Lewandowski et al. [11].

$$Nu = 0.774 Ra^{\frac{1}{5}} \tag{5}$$

where:
Nu – Nusselt number,
Ra - Rayleigh number.

At the vertical edge of the plate, and at the vertical surface cooled under natural convection, the HTC was calculated from formula developed by Churchill and Chu [13].

$$Nu = \left\{ 0.825 + \frac{0.387 Ra^{\frac{1}{6}}}{\left[1 + \left(\frac{0.492}{Pr}\right)^{\frac{9}{16}}\right]^{\frac{8}{27}}} \right\} \tag{6}$$

where:
Pr – Prandtl number.

The boundary condition at the vertical plate surface cooled by the air nozzle has been approximated by the product of functions

$$\propto_{con} (\ \dot{w}, T_s, H_N, p) = \dot{w}\,(x_2, x_3, H_N, p)^{Awp} D(T_s, H_N, p) \tag{7}$$

where:
Awp – Parameter regulating the air flux distribution,
D – Thermal characteristic of air $[J/(kg \cdot K)]$,
H_N – Distance from nozzle to surface $[m]$,
p – Air pressure $[Pa]$,
$\dot{w}$ – Air flux $[kg/(s \cdot m^2)]$,
$\propto_{con}$ – Convection heat transfer coefficient $[W/(m^2 \cdot K)]$.

The function D depends on a local temperature T_s of the plate surface, air pressure p, and the nozzle distance to surface H_N. For a particular air pressure p and the nozzle distance to surface H_N the function D depends only on the plate surface temperature T_s. A scheme of the function D approximation has been shown in (Fig. 5). The plate surface temperature from the plate initial temperature T_0 to the air temperature T_a has been divided into 5 sections. The beginning, and the end of a particular section k is defined by the temperature T_k and T_{k+1}, respectively. The value of the function D at point T_k is defined by D_k parameter. However, for the plate surface temperature equal to the air temperature the convection HTC vanishes and therefore $D1 = 0$. The remaining D_k parameters for $k = 1$ to 5 must be determined from the minimum condition of the objective function (15).

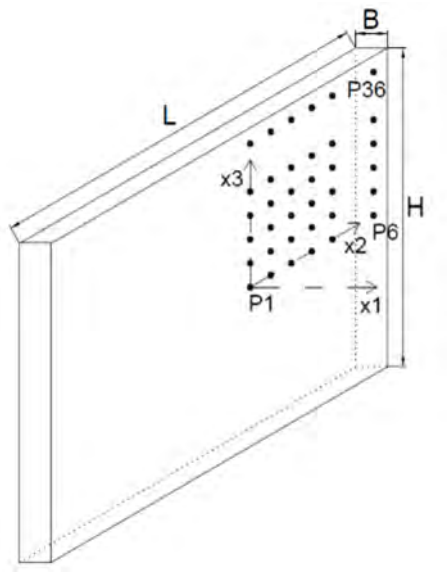

Figure 4: The arrangement of thermocouples

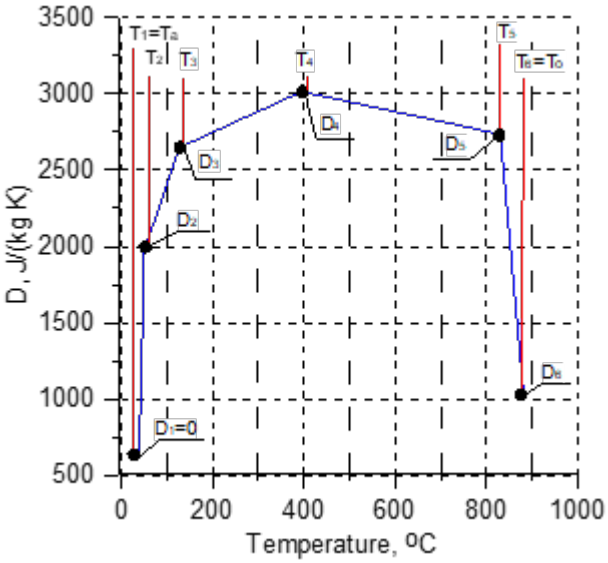

Figure 5: Scheme of thermal characteristic of air as a function of the plate surface temperature.

For surface temperature $T_a < T_s < T_2$ dimensionless temperature η is defined as

$$\eta = \frac{T_s - T_a}{T_2 - T_a} \tag{8}$$

and the function D is calculated from

$$D(\eta) = D_2\, \eta^2 \tag{9}$$

For surface temperature$T_s > T_2$ and $T_k < T_s < T_{k+1}$ dimensionless temperature η is defined as

$$\eta = \frac{T_s - T_k}{T_{k+1} - T_k} \tag{10}$$

and the function D is calculated from

$$D(\eta) = D_k\,(1-\eta) + D_{k+1}\,\eta \tag{11}$$

The function $\dot{w}\,(x_2, x_3, H_n, p)$ describes the rate of air flow over the cooled surface in $kg/(s \cdot m^2)$.

The local air flux has been determined on the basis of measurments that were done for water-air nozzle described in [14]. These measurments allowed to develop the hydraulic characteristic of the MNM nozzle. Distribution of air flux rate has been approximated in cylindrical coordinates using nondimensional distance from the stagnation point r_z:

$$r_z = c_1\, \frac{150}{H_N} \sqrt{x_2^2 + x_3^2} \tag{12}$$

The parameter r_z defines dimensionless radius at which air moving along the conical surface of the spray touches the plate regardless of the nozzle position HN. For the axially symmetrical approximation of the measured air flux two functions given by Eq. (13) and Eq. (14) have

been selected. The function defined by Eq. (13) approximates the air flux distribution from the stagnation point to a position $r_z = 1$:

$$\dot{w}\,(r, H_N, p) = 0,55 \left(\frac{150}{H_N}\right)^2 p^{c_5}\,(1 + c_2\ r_z^{c_3}) \exp\,(-r_z)\ \ for\ \ r_z\ \leq 1 \tag{13}$$

The function defined by Eq. (14) approximates the air flux distribution from a point $r_z = 1$ to infinity:

$$\dot{w}\,(r, H_N, p) = 0.55 \left(\frac{150}{H_N}\right)^2 p^{c_5}\,(1 + c_2\ r_z^{c_4})\, exp\,(-r_z^{c_4})\ \ for\ r_z \geq 1 \tag{14}$$

Nozzle Angle	Coefficient				
	c_1	c_2	c_3	c_4	c_5
45°	0.0512	0.1870	0.0000	1.0000	0.4800

Table 2: Coefficients employed in Eq. (12), Eq. (13) and Eq. (14) for a MNM nozzle angle of 45°.

It is important to notice that at point $r_z = 1$ the air flux calculated from Eq. (13), or Eq. (14) has the same value. The air flow rate calculated as the integral of Eq. (13) and Eq. (14) over the range from $r = 0$ to $r = 150mm$ was in a good agreement with the rotameter indication given in Table 1.

The parameters D_i and the Awp parameter defining the D function distribution have been obtained by minimizing the objective function:

$$E(D_i, Awp) = \frac{1}{NT \cdot NP} \sum_{m=1}^{NT} \sum_{n=1}^{NP} \left[\frac{1}{\sqrt{1 + \left(\frac{\Delta Te^{nm}}{\Delta \tau}\right)^2}} (Te^{nm} - T(D_i, Awp)^{nm}) \right]^2 \tag{15}$$

where:

Te^{nm} – Sample temperature measured by the sensor n at the time τ_m,

T^{nm} – Computed sample temperature at the location of the sensor n at the time τ_m,

NP – Number of temperature sensors,

NT – Number of temperature measurements performed by one sensor.

The objective function (15) defines the temperature difference between measured and computed temperatures along the normal to the measured temperature curve.

The radiation heat losses depended on the plate emissivity $\varepsilon_s(T)$ has been calculated from the emissivity model developed based on inverse solution to the Armco plate cooling under natural convection in air:

$$\varepsilon_s = 0.5 + 0.35\ \bar{t}_p^2 \tag{16}$$

4 IDENTIFICATION OF THE HEAT TRANSFER COEFFICIENT

The performed numerical calculations made it possible to determine the local convection HTC on the cooled surface of the Armco plate covered with scale. In Fig. 6 and Fig. 7, local HTC distributions in relation to the surface temperature excess, and time, respectively, calculated at 6 elements E1-E6 have been presented. The centers of the elements, in which the local HTC have been presented, corresponded to the positions of P1, P2, ..., P6 thermocouples inserted along x_2 axis (Fig. 4). In Fig. 8 the thermal characteristics of air versus the temperature excess has been presented.

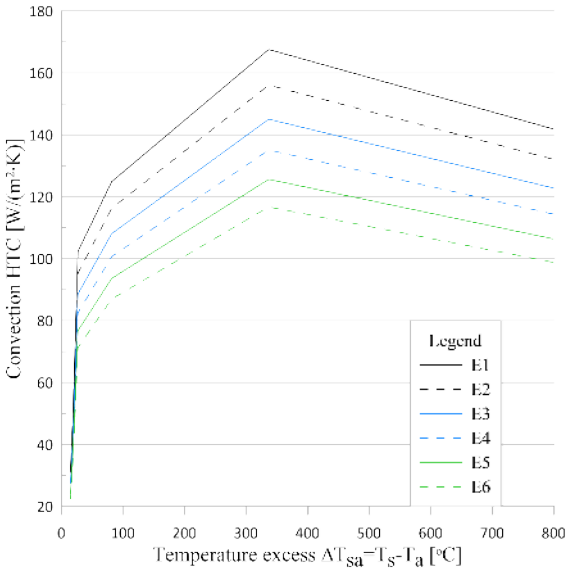

Figure 6: The local convection HTC distributins versus the temperature excess.

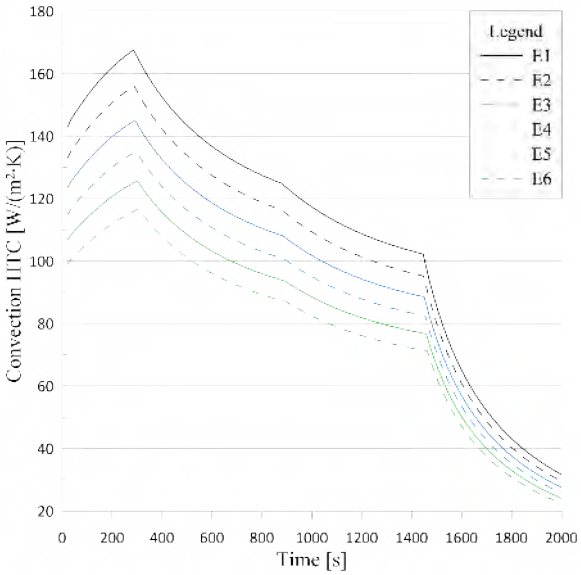

Figure 7: The local convection HTC distributions versus the time of cooling.

From the beginning of the air nozzle cooling, the convection HTC increase during about 300 s and reaches the maximum value depending on the location along x_2 axis (Fig. 7). The lowest value of a maximum convection HTC of $115W/(m^2 \cdot K)$ was reached at element E6, and a highest of $165W/(m^2 \cdot K)$ at element E1. It is related to the air velocity and mass flux. Near the center of the nozzle axis, the air velocity as well as the air mass flux are the highest. It increases the convection heat transfer process. As the distance from the nozzle axis increases, the air mass flux decreases. During the first 300 s of cooling process carried out with the air nozzle, the plate temperature decreases to about $350°C$ (Fig. 6). During that time the HTC has reached the maximum values, Next, the convection HTC decreases gradually, and after subsequent 1100 s has reached about $130W/(m^2 \cdot K)$ in E1, and $90W/(m^2 \cdot K)$ in E6 (Fig. 7). During this time, the plate temperature decreases slowly from $350°C$ to about $120°C$ (Fig. 6). In the last stage of cooling which lasted of about 600 s, a rapid drop in convection HTC values was observed.

In Fig. 8 the thermal characteristics of the air has been shown. This characteristic is presented as a function that determines the ability of a coolant to remove heat from the cooled surface. Such presentation of the results allows to eliminate the influence of the amount of air supplied on the efficiency of the cooling process. As shown in Fig. 8, the greatest ability of heat extracting from the cooled surface was obtained in element E1, which was located in the axis of the air stream. As the distance from the nozzle axis increases, the ability of heat removing decreases (Fig. 8). Such a behavior is related to the distribution of air velocity and the air mas flux distribution over the cooled surface.

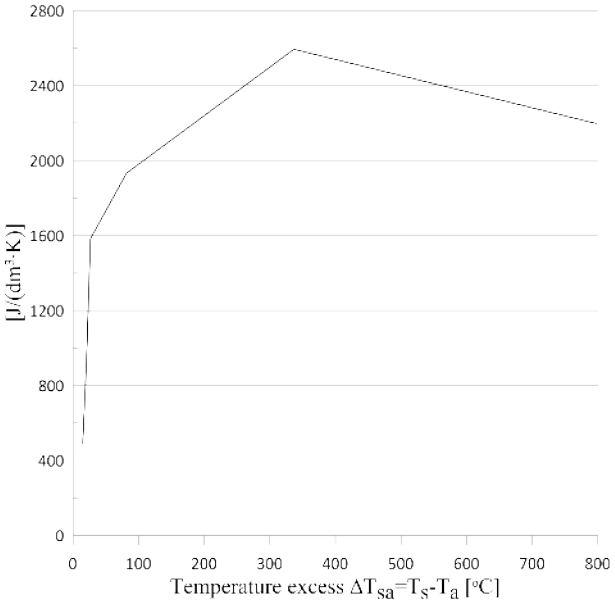

Figure 8: Function defining thermal characteristic of air versus the surface temperature excess.

The accuracy of the performed inverse solutions to the convection HTC identification has been presented in Table 3. The average temperature difference between measured and calculated temperature did not exceed 2K. This indicates a satisfactory accuracy of the numerical calculations.

Average deviation	Maximum negative deviation	Maximum positive deviation
[K]	[K]	[K]
1.667	-5.95	7.88

Table 3: Inverse solution accuracy

5 CONCLUSION

The inverse solution to the heat conduction equation for the heat transfer coefficient determination during the vertical plate cooling by the air nozzle has been obtained. Three-dimensional heat conduction problem has been solved using the finite element method. The thermophysical properties of the Armco steel have been considered as functions of temperature. The oxide layer on the cooled surface has been considered in the heat conduction model as well. The thickness of the oxide layer of about 0.1 mm has been determined based on the oxidation process kinetics. The boundary condition at the oxide layer has been defined. The boundary condition model has been specified as a product of two functions. The first function defined the air flux specific for a particular nozzle. The second function defined the air ability to extract heat from the cooled surface. The parameters of the heat conduction model were determined from the minimum condition of the object function. It has been found that the convection heat transfer coefficient increases rapidly as the plate temperature grows. However, the convection heat transfer coefficient has reached a maximum value at the plate temperature of $350°C$. For the plate temperature range from $350°C$ to $800°C$ a linear decrease in the HTC has been obtained. Air flux distribution over the cooled surface is a particularly important in the developed boundary condition model.

FOUNDING

Scientific study financed from the regular activity of the Faculty of Metals Engineering and Industrial Computer Science of AGH University of Science and Technology.

REFERENCES

[1] Yang L., Ren J., Jiang H., Ligrani P., Experimental and numerical investigation of unsteady impingement cooling within a blade leading edge passage, International Journal of Heat and Mass Transfer, Vol. 71, 2014, pp. 55-68

[2] Dou R., Wen Z., Zhou G., 2D axisymmetric transient inverse heat conduction analysis of air jet impinging on stainless steel plate with finite thickness, Applied Thermal Engineering, Vol 93, (2016), pp. 468-475

[3] Guo Q., Wen Z., Dou R., Experimental and numerical study on the transient heat-transfer characteristics of circular air-jet impingement on a flat plate, International Journal of Heat and Mass Transfer, Vol. 104, 2017, pp. 1177-1188

[4] Beck J.V, Nonlinear estimation applied to the nonlinear inverse heat conduction problem, International Journal of Heat and Mass Transfer 13, 1970, pp. 703-716

[5] Malinowski Z., Telejko T., Hadała B., Cebo-Rudnicka., Szajding A., Dedicated three dimensional numerical models for the inverse determination of the heat flux and heat transfer coefficient distributions over the metal plate surface cooled by water, International Journal of Heat and Mass Transfer, (2014), Vol. 75, pp. 347-361

[6] Lee H-L., Chang W-J., Wu S-Ch., Yang Y-Ch., An inverse problem in estimating the base heat flux of an annular fin based on the hyperbolic model of heat conduction, International Communication in heat and Mass Transfer, Vol 44, (2013), pp. 31-37

[7] Li M., Endo R., Akoshima M., Susa M., Temperature Dependence of Thermal Diffusivity and Conductivity of FeO Scale Produced on Iron by Thermal Oxidation, ISIJ International, Vol. 57, (2017), No. 12, pp. 2097-2106

[8] Maachou A., Malti R., Melchior P., Battaglia J-L., Oustaloup A., Hay B., Application of fractional Volterra series for the identification of thermal diffusion in an ARMCO iron sample subject to large temperature variations, IFAC Proceedings Volumes, Vol. 44, Issue 1, (2011), pp. 5621-5626

[9] Polska Norma PN-EN 60584-2: 1997 Termoelementy. Tolerancje

[10] Data acquisition system MGCplus datasheet, Hottinger Baldwin Messtechnik,

[11] Shanks H. R., Klein A., H., Danielson G. C., Thermal Properties of Armco Iron, Journal of Applied Physics, Vol. 38, (1967), pp. 2885-2892

[12] Lewandowski W. M., Radziemska E., Buzuk M., Bieszk H., Free Convection heat transfer and fluid flow above horizontal rectangular plates, Applied Energy, Vol. 15, (1972), pp. 2535-2549

[13] Churchill S.W., Chu H. H. S., Correlating equations for laminar and turbulent free convection from a vertical plate, Int. Journal of Heat and Mass Transfer, Vol. 18, (1975), pp. 1323–1329

[14] Cebo-Rudnicka A., Malinowski Z., Identification of heat flux and heat transfer coefficient during water spray cooling of horizontal copper plate, Int. Journal of Thermal Sciences, Vol.145 (2019), pp. 1-24